第８回地震時保有耐力法に基づく橋梁等構造の
耐震設計に関するシンポジウム講演論文集（2005 年 2 月）

A CODE-BASED COMPARATIVE STUDY ON RC DEEP BEAMS BEHAVIOR WITH SHEAR SPAN TO DEPTH RATIO BETWEEN 0.5 AND 1.5

MOHAMMAD REZA SALAMY[1], HIROSHI KOBAYASHI[2], SHIGEKI UNJOH[3], KENJI KOSA[4], TSUTOMU NISHIOKA[5]

[1]Member of JSCE, Dr. of Eng., Public Works Research Institute, Earthquake Engineering Research Team
Earthquake Disaster Prevention Research Group, Minamihara 1-6, Tsukuba-shi, Japan 305-8516
[2]Member of JSCE, Public Works Research Institute, Earthquake Engineering Research Team
[3]Member of JSCE, Dr. of Eng., Public Works Research Institute, Leader of Earthquake Engineering Research Team
[4]Member of JSCE, PhD, Kyushu Institute of Technology
[5]Member of JSCE, Dr. of Eng., Hanshin Expressway Public Corporation

1. Introduction

In order to investigate RC deep beams behavior and lateral reinforcement effects in improving shear behavior of those beams, a study is undergoing in Public Works research Institute (PWRI) based on the experiments conducted during the year 2003 and 2004. Three sets of specimens comprise of nineteen RC beams including the experiments carried out on a joint research basis with Kyushu Institute of Technology (KIT) and Hanshin Expressway Public Corporation (HEPC) are investigated in this study. The beams have shear span to depth ratio between 0.5 and 1.5 and effective depth size from 400 mm to 1400 mm. The longitudinal tensile reinforcement ratio is kept almost constant in about 2% for all specimens while lateral reinforcement (stirrups) ratio varies by 0.0%, 0.4% and 0.8% in shear span. The results of experiment compared with Japanese design code such as Japan Road Association[1, 2] (JRA) and Japan Society of Civil Engineers[3] (JSCE). In order to trace compressive force path in RC beams, numbers of acrylic bars are located in between loading plates and supports to measure strain in concrete in the designated path. The objective of using this method in experiment is to verify the validation of strut-tie model and also characterize and measure actual strain in the location with highest possibility of crushing or cracking in any kind of shear failure occurs in RC beams with low a/d ratio. The results presented in this paper are part of a larger study on shear behavior of RC deep beams including size effect experimentally and numerically. In this regard, only experimental results in comparison with codified design results. It is found however that by increasing a/d in both design-codes, shear strength of the member will be decreased which agree well with experimental observation. On the other hand, JRA code yields better prediction in comparison with JSCE with an adequate safety margin.

2. Experiment setup and specimens details

To evaluate analytical results of FEM as well as code-based design, the following sets of experiments are carried out at PWRI and Kyushu Institute of Technology. However analytical evaluation by FEM will be presented in future in some other publications and here only the

Table 1: Steel Properties of specimens

Beam	ρ_w %	ρ_{st} %	f_y *MPa*	Ast Asc	Stirrups
B-2	0.0	2.02	376	5D22 2D10	
B-3	0.4				D6@65
B-4	0.8				D10@75
B-6	0.0				
B-7	0.4				D6@65
B-8	0.8				D10@75
B-10-1	0.0				
B-10-2					
B-11	0.4				D6@65
B-12	0.8				D10@75
B-10.3-1	0.0	2.11	388	9D25 2D16	
B-10.3-2			371.7		
B-13-1	0.0	2.07	398	10D32 2D13	
B-13-2					
B-14	0.0	2.04	398	14D32 4D13	
B-17	0.4				D13@100
B-15	0.0	1.99	402	18D35 2D13	
B-16	0.0	2.05	394	18D41 2D13	
B-18	0.4		397.5		D16@120

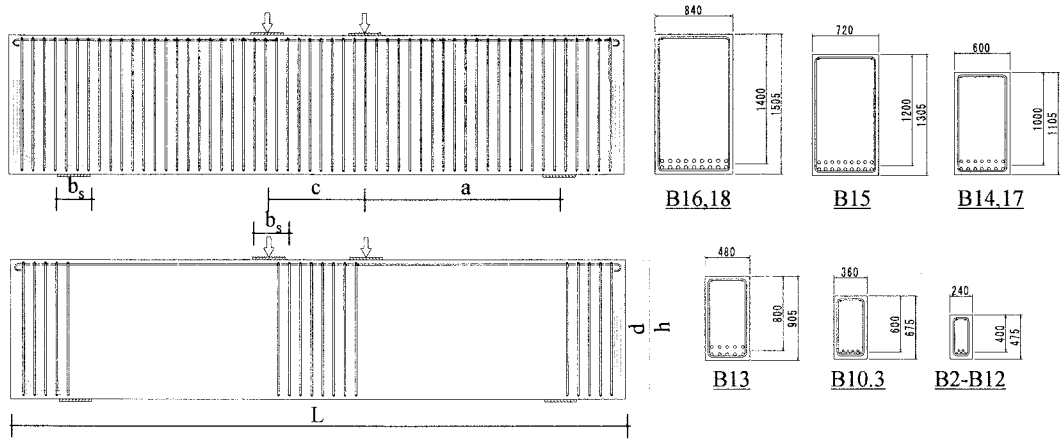

Fig.1. Detail of specimens with and without stirrups

results of design codes are evaluated by experimental observation. Experiments consist of nineteen RC beams with geometric characteristic and material properties given in Fig.1, Table 1 and Table 2.

In Table 1, ρ_w, ρ_s, f_y, A_{st} and A_{sc} are shear span, stirrups ratio, longitudinal tensile reinforcement ratio and their yield stress, cross section area of tensile and compressive reinforcement respectively. All specimens, with or without stirrups in shear span, have a minimum lateral reinforcement in mid-span and out of span. Despite absence of shear stress in this part, which in the first look implies un-necessities of shear reinforcement, they may delay or in some case prevent the propagation of diagonal crack to compression zone. It is believed even that reinforcements in mid-span sometimes are more effective than those in shear span due to the reason stated above[4]. Further study is however necessary to confirm the effect of mid-span stirrups experimentally.

In Table 2, b is specimen width, a/d and f_c' are shear span to depth ratio and compressive stress respectively. Maximum load capacity and related deflection as well as shear crack initiation load and maximum deflection are noted as $P_{\max}$, P_{cr}^{sh}, δ_{peak} and $\delta_{\max}$ respectively. Other geometrical parameters of Table.2 are schematically determined in Fig.1. All specimens are subjected to four points monotonic static load condition. Experimental data acquisition is mainly focused on mode of failure; crack patterns, load-displacement relationship as well as steel and concrete strain in some designated locations to evaluate the analytical results.

Table 2: Geometric and material Properties of specimens

Beam	a/d	Geometry size (mm)							f_c' *MPa*	$P_{\max}$ KN	P_{cr}^{sh}	δ_{peak} *(mm)*	Failure Mode
		L	c	a	d	h	b	b_s					
B-2	0.5	700	300	200	400	475	240	100	36.2	1550	525	3.16	II
B-3										1536	625	4.78	II
B-4									31.3	1951	700	1.85	II
B-6	1.0	1100		400					31.3	1050	400	2.77	II
B-7										1181	400	2.83	II
B-8									37.8	1501	600	3.26	II
B-10-1	1.5	1500		600					29.2	616	325	3.82	II
B-10-2									23	703	278	5.28	II
B-11									29.2	1025	350	15.96	II
B-12									31.3	1161	300	7.05	II
B-10.3-1		2250	450	900	600	675	360	150	37.8	1960	700	6.62	II
B-10.3-2									31.15	1787	527	8.62	II
B-13-1		3000	600	1200	800	905	480	200	31.63	2985	500	11.87	II
B-13-2									24	2257	807	9.33	II
B-14		3750	750	1500	1000	1105	600	250	31	3969	1100	9.27	II
B-17									28.7	5214	1600	11.92	II
B-15		4500	900	1800	1200	1305	720	300	27	5390	1500	11.91	II
B-16		5250	1050	2100	1400	1505	840	350	27.3	5975	1900	10.57	II
B-18									23.5	8396	2400	15.79	II

3. Shear failure mechanism of RC beams

Failure modes are so determined in two main categories of flexural failure mode (Mode I) and shear failure mode (Mode II) with three subcategories for Mode II failure as followings:

Mode II-1: Diagonal tension failure, which in the line of thrust become so eccentric and give rise to flexural failure in compressive zone. It is important however to mention that this kind of failure is a result of tensile crack extension in compressive zone due to the flexural load.

Mode II-2: Shear compression failure where RC beam fails due to the development of diagonal crack into the compressive zone and reduces the area of resisting region excessively and beam crushes once generated compressive stress exceed compressive strength of concrete.

Mode II-3: Shear proper or compressive failure of struts, which is often observed in beams with very small shear span to depth ration a/d (about a/d<1.5). In this case due to the small a/d ratio, the line of thrust will be so steep and arch action not only reserve flexural capacity in most cases but also efficiently sustains required shear force. Arch formation is clearly observed in those beams and finally beams fail due to either sudden tensile crack formation parallel to the strut axes or compressive crush in normal direction to the strut axes. The latter case shows more reserved load after crushing (for instance Beams 13, 10.3 and B18). Figure 2 depicts crack pattern of B-18 at the last stage of loading where the beam failed as a result of strut compressive failure in the location stated in the figure. Thrust zone is schematically shown in this figure. Despite compressive failure in strut the beam sustained almost 80% of peak load and a plateau formed after small drop of the peak load. This phenomenon happened in some other beams such as B17 and B15, which is in contrary to what shear failure naturally implies as a sudden failure. Some results for specimens with large reserved load capacity after peak load are shown in figure 3. Note however that concrete is a rate dependent material so loading rate is supposed to have significant effect on RC member behavior and should be taken into account when numerical simulation is performed.

It is also worth to note that arch action requires a substantial horizontal reaction at the support to be formed. To satisfy this condition tensile bars in all specimens are well anchored with a rather long hook beyond support region. In this study only the effect of shear span stirrups have been considered though it would be of interest to study on influence of stirrups in mid-span in preventing diagonal crack to compressive zone for larger a/d ratios.

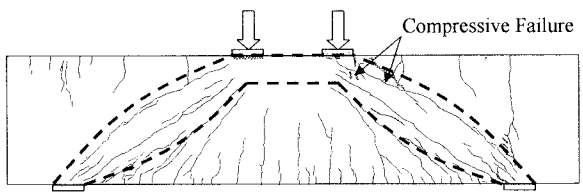

Fig.2. Crack Pattern of Beam 18

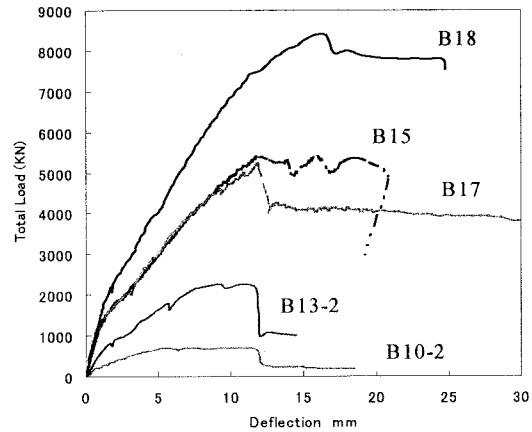

Fig.3. Experimental results of beams with large load reserve after peak load.

4. Design codes proposed equations for shear strength of RC members

Design codes JSCE (Japan Society of Civil Engineers) and JRA (Japan Road Association) are employed to design tested beams for comparison with experiment by means of shear span to depth ratio as well as effective depth size effect. Since JRA code is not formulized like other codes and design values are presented in a tabular form, here only shear design procedure of JSCE code is presented briefly. It is noted however that JRA design code henceforth means design through part five[2] taking into account the effect of deep beam (C_{dc} and C_{ds}) through part four[1] (page 230).

JSCE code: Based on this code, shear capacity of concrete in RC members V_{cd} (concrete contribution to shear capacity) can be obtained by the following equations. L and h are beam's span and height.

In case of $\frac{L}{h} \geq 2$ for simple beams:

$$V_{cd} = \frac{\beta_d \beta_p \beta_n f_{vcd} b_w d}{\gamma_b} \quad (1)$$

$$\beta_d = \sqrt[4]{\frac{1000}{d}} \leq 1.5 \quad (2)$$

$$\beta_p = \sqrt[3]{100 \rho_s} \leq 1.5 \quad (3)$$

$$\rho_s = A_s / (b_w . d) \quad (4)$$

$$f_{vcd} = 0.2 \sqrt[3]{f'_{cd}} \leq 0.72 \quad (N/mm^2) \quad (5)$$

Parameters A_s, f'_{cd}, γ_b, b_w and d are longitudinal tensile reinforcements area, concrete ultimate compressive stress, uncertainty parameter which in general case will be 1.3, member web width and effective depth in critical section respectively. Since the nominal shear strength is used for comparison with experiments, $\gamma_b = 1$ is supposed to set in all calculation. However the parameter for material uncertainty is not explicitly stated in JRA

code therefore to have a meaningful comparison between two codes $\gamma_b = 1.3$ is conducted. On the other hand experimental results are also calibrated by the same reduction factor equal to 1.3. The value $\beta_n = 1$ is also adopted due to the code definition for simply supported beams.

In case of $\frac{L}{h} < 2$ for simple deep beams:

$$V_{cd} = \frac{\beta_d \beta_p \beta_a f_{dd} b_w d}{\gamma_b} \quad (6)$$

$$f_{dd} = 0.19\sqrt{f'_{cd}} \quad (N/mm^2) \quad (7)$$

$$\beta_a = \frac{5}{1+(a/d)^2} \quad (8)$$

$$\phi = -0.17 + 0.3(a/d) + 0.33/\rho_{wb} \le 1.0 \quad (9)$$

$$V_{sdd} = \phi . V_{sd} \quad (10)$$

$$V_{sd} = \frac{A_w f_{wyd} (\sin\alpha_s + \cos\alpha_s)/s_s}{\gamma_b} . z \quad (11)$$

where $z \approx d/1.15$ and $f_{wyd} \le 400 MPa$ for normal strength concrete. Lateral reinforcement contribution to shear capacity is denoted by V_{sd} and is calculated by Eq.11 for any values of $\frac{L}{h}$ ratio.

Finally the shear capacity of entire section V_{yd} is calculated through Eq.12 as below.

$$V_{yd} = V_{cd} + V_{sdd} \quad (12)$$

5. Comparison of the Results

Both codes are applied for shear load capacity calculation. The results of codified calculation and experimental observation are shown in figures of this section.

(1) Load capacity

As mentioned in section 4, only simply supported beams with L/h<2 are considered as deep beam by JSCE design code. In other words despite most other design codes including JRA which recognize beams with a/d<2.5 as deep beam, only the specimens tested in this study with a/d=0.5 are recognized by JSCE code as deep beam. Nevertheless in this study, beams are designed in both cases of only following JSCE regulation as well as considering all beams as deep beams and applying JSCE deep beam criterions.

Figures 4 and 5 show ultimate loads of specimens along with those obtained by the mentioned design codes. Dotted lines in figures illustrate reduced ultimate loads by means of JSCE reduction factor $\gamma_b = 1.3$ to calibrate test results for the sake of comparison with reduced design codes predictions. As can be seen in both figures, JRA code gives much better agreement to the experiment than JSCE code with an acceptable safety margin. JSCE code seems however has no consistency in terms of deep beam

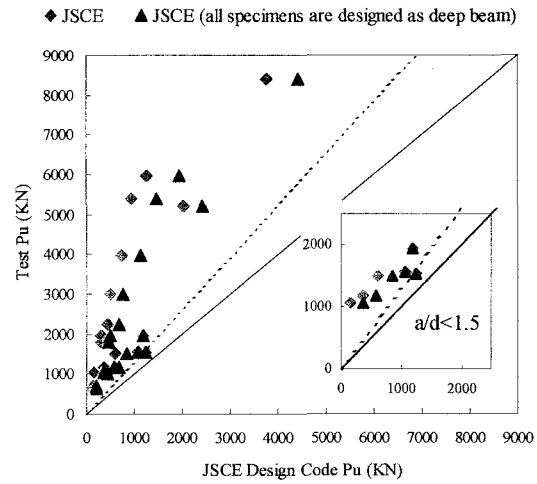

Fig.4. JSCE design code ultimate load versus test result

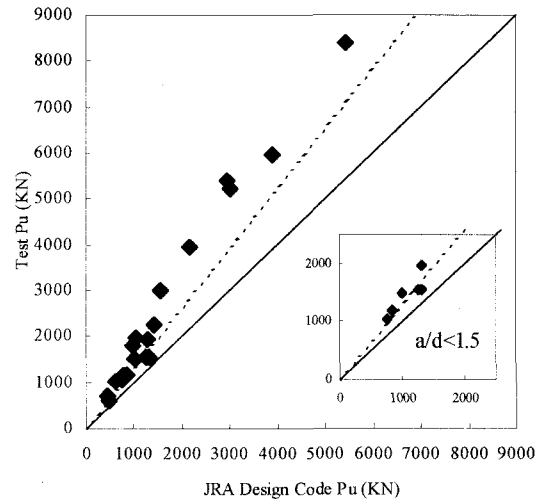

Fig.5. JRA design code ultimate load versus test result

definition and the results show a kind of scatter distribution around both solid and dotted lines. It is however observed that no data points fall significantly below either lines for any of the codes. Experiment showed that shear crack initiated at about 40% of the ultimate load and full shear crack will be formed approximately in $0.5P_u$ but still beam sustained load capacity to about 80-90% of the ultimate load. Afterward shear cracks were severely widened and extended to compressive zone. Shear sliding of concrete pieces around shear crack could be clearly observed with bare eyes. This point is considered the ultimate capacity of beam in shear by a number of design codes, which the beam is in serious irreversible circumstances. Aggregate interlock, which is the backbone of current codes are almost exhausted in this stage. Figure 6 shows code prediction capacities in terms of above-mentioned proportions to the experiment peak load.

The figure shows that JSCE code have usually estimated the load capacity of members around shear crack initiation load while JRA code yields the results near practical ultimate capacity of beams (about 0.8Pu). In other words, for beams with a/d>0.5 JRA allows shear

crack occur and extend but JSCE allows only shear crack form but not extend. It is acceptable in essence if the philosophy of JSCE code like some other design codes is to ensure the safety of structures before initiation of shear cracks not to reach to the ultimate load. Nevertheless the discrepancy in the results is for beams with a/d<1.0 which gave rise to a jump in predicted shear capacity of the member by JSCE and despite a big safety margin for specimens with larger a/d ratio, these beams seem to be overestimated. Figure 7 gives a comparison between load capacity observed in experiment and design codes. For a/d=0.5, JSCE and JRA yield almost same prediction but two codes differ more as long as a/d increases. Shear crack load is also presented in this figure to clarify and follow the discussion made on figure 6. On the other hand, complementary JSCE standard specification[4] present a rigorous procedure in design of deep beams with a/d<3. Equations 1 to 5 are applied for design while a new coefficient taking into account the effect of a/d ratio as follows.

$$\beta_a = 0.75 + \frac{1.4}{a/d} \qquad (13)$$

Effect of β_a is illustrated in figures 8 and 9. Although the results show better agreement with experiment and also clod to JRA prediction but for beams with a/d=0.5 load capacity goes beyond experiment load even with no reduction factor.

(2) Size effect

In order to study size effect in shear capacity of beams with low a/d ratio, both code examined and verified with experimental results. Test specimens cover a wide range of effective depth from 400mm to 1400mm. Accordingly variation of average shear stress taking into account concrete compressive strength ($V_u / b.d.\sqrt[3]{f_c'}$) in terms of effective depth is shown in figure 10. To eliminate a/d effect on ultimate shear stress of the beams, only a/d=1.5 is considered here. It is clear that as long as the effective depth increases, the shear strength of the section decreases. The regression curve is assumed to be a power function of effective depth d in order to adjust to the size effect function proposed by JSCE and JRA. The equation is round off and rewritten in the following form

$$f(v_u) = \lambda(d^{-0.22}) \qquad (14)$$

where coefficient λ is a function of a/d ration, reinforcement ration and member's boundary condition. Since the three aforementioned parameters are constant for the beams used for producing figure 10 consequently $\lambda = 4.77$ is determined to best fit to the experiment data points. According to JSCE, shear stress varies in a form given by Eq.2 in terms of $d^{\frac{1}{4}}$. On the other hand JRA[1] proposed procedure can be estimated by a function of $d^{\frac{1}{3}}$ to take into account size of specimen. Although the foregoing expression of figure 10 is a crude

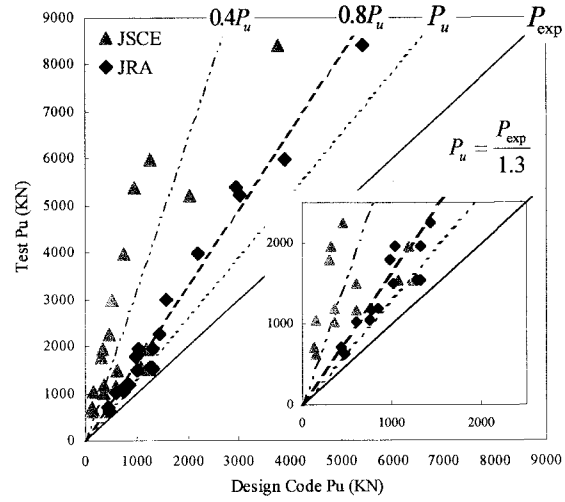

Fig.6. Design code ultimate load versus test result

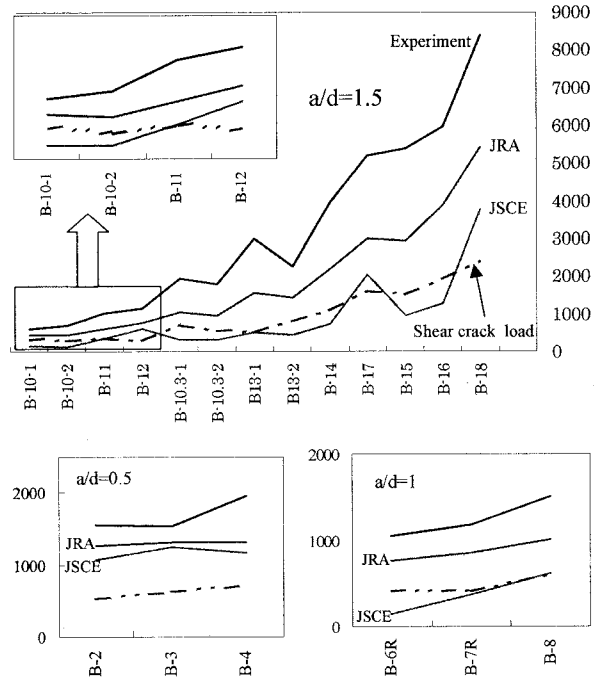

Fig.7. Experiment and design code load for all specimens

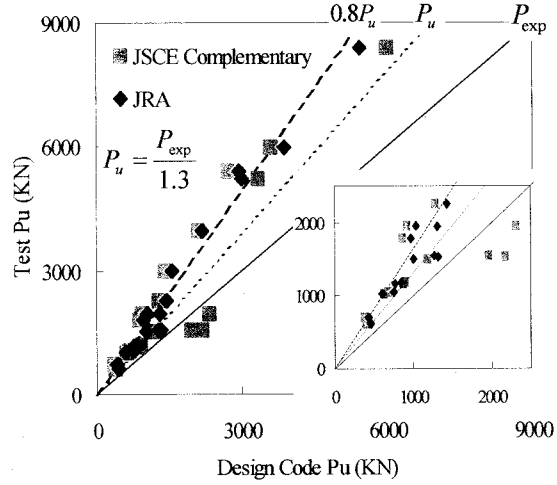

Fig.8. Design code ultimate load versus test result

approximation, the form of equation 14 agrees well with that of Eq.12 of JSCE code. It is however not a significant differences between JSCE and JRA size effect expression as can be seen in figure 11 and both expressions are attributed to a reasonable estimation of member depth effect. The maximum values for this coefficient set 1.0 and 1.5 by JRA and JSCE code respectively. In other words, in spite of JSCE code, which attributes 50% increase in shear strength capacity to size effect, JRA however does not allow any increase in shear strength. One reason for this might be the fact that JRA is usually dealing with structures with large components most of them larger than one-meter depth but JSCE should cover wider range of element size since it is to design various structures too.

6. Conclusion

A comparative study between experiment, JSCE and JRA design codes has carried out by means of ultimate loads, shear crack loads as well as size effect issues proposed by either codes. It is found that JRA code has a consistence design procedure for RC beams with low shear span to depth ratio. This code assumes beams with a/d<2.5 as deep beams while JSCE has larger limit for deep beam as L/h<2 where L and h are beam's span and height respectively (more than two time bigger than JRA limit). Therefore only beams with a/d=0.5 of this experiment are designated by JSCE to follow the deep beam design procedure. Since deep beams usually have higher shear strength due to the resisting mechanism of such beams against external loads by means of compressive arch formation, there will be a discrepancy between experimental observation and estimated strength by JSCE code. Estimated shear load capacity by JSCE is around shear crack load of experiments while JRA code allows shear cracks form and extend to a certain level with higher load capacity prediction. In this sense it can be concluded that JSCE design code yields much conservative results than that of JRA except for very small a/d ratio say 0.5 where JSCE amplifies the predicted shear strength by means of a function of a/d ratio (Eq.8). It is noted however that no code data points go beyond experiment ultimate loads. Application of Complementary JSCE standard specification is also examined for tested beams. Despite better agreement with experiment and closer results to JRA prediction, data points for a/d=0.5 drop below the line (Fig.8) or in other words, predicted load capacity goes beyond obtained load by experiment.

Concerning size effect in shear strength of RC beams with low a/d ratio, experimentally observed size effect by means of effective depth variation confirmed that both code have included this phenomenon in design procedure adequately thought JSCE equation has better agreement with experiment. The main difference between the codes lies on the beams with depth smaller than 1000mm which JRA limits the coefficient to one but JSCE goes as far as 1.5 and attributes shear strength to the size effect up to 50% higher in members with depth less than one meter.

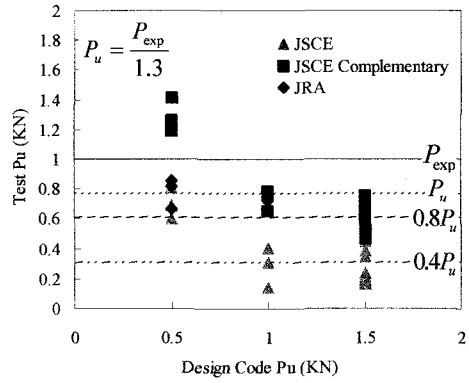

Fig.9. Design code ultimate load to test ratio versus a/d

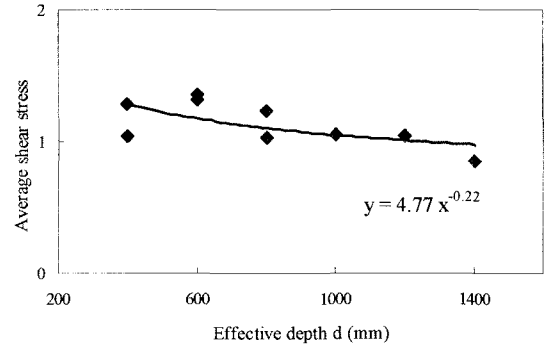

Fig.10. Effective depth versus $V_u / b.d\sqrt[3]{f'_c}$ for Av=0 and a/d=1.5

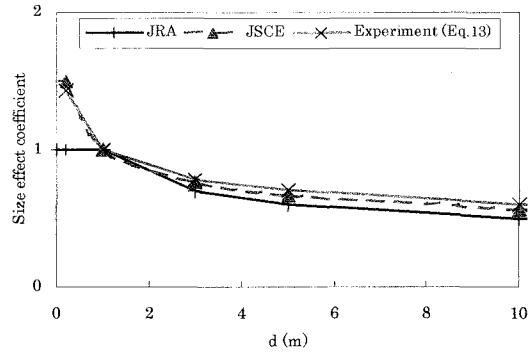

Fig.11. Effective depth versus size effect coefficient

REFRENCES

1. Japan Road Association. *Design specifications of highway bridges. Part IV: substructures;* (in Japanese), 2002.
2. Japan Road Association. *Design specifications of highway bridges. Part V: seismic design*; (in Japanese), 2002.
3. Japan Society of Civil Engineers. *Standard specifications for concrete structures-2002, Structural performance verification.* March 2002, Tokyo, Japan (in Japanese).
4. Behavior of Reinforced Concrete Beams with a Shear Span to Depth Ratio Between 1.0 and 2.5, Michael D. Kotsovos, ACI Journal, May-June 1984
5. Japan Society of Civil Engineers. *Complementary for standard specifications for concrete structures-2002,* March 2-002, Tokyo, Japan (in Japanese).